Lab on a Chip

Cite this: DOI: 10.1039/c2lc40948h

www.rsc.org/loc

TECHNICAL INNOVATION

Luminometric sub-nanoliter droplet-to-droplet array (LUMDA) and its application to drug screening by phase I metabolism enzymes†

Giuseppe Arrabito,[a] Clelia Galati,[b] Sabrina Castellano[c] and Bruno Pignataro*[d]

Received 19th August 2012, Accepted 25th October 2012
DOI: 10.1039/c2lc40948h

Here we show the fabrication of the Luminometric Sub-nanoliter Droplet-to-droplet Array (LUMDA chip) by inkjet printing. The chip is easy to be implemented and allows for a multiplexed multi-step biochemical assay in sub-nanoliter liquid spots. This concept is here applied to the integral membrane enzyme CYP3A4, *i.e.* the most relevant enzymatic target for phase I drug metabolism, and to some structurally-related inhibitors.

In the last decade, due to the advancements in the -omics sciences, an integrated investigation of living systems at a molecular level has become possible. In order to fully benefit from this scenario, innovative, low-cost, small-volume, solution-based screening methods are necessary to address such issues of growing biological complexity.[1] Conventional miniaturized screening methodologies – based on robotic dispensers coupled with microwell arrays – involve time and reagent consuming (micro-, nanoliter scale volumes) instrumental tools as well as expensive facilities. Thus, simplifications of the experimental set-up, cost reduction, and further miniaturization are all highly required features especially in fields like drug discovery.[2] To address these issues, it is decisive to take advantage from both knowledge on supramolecular self-assembly processes allowing for ordered nano- and/or micro-scale structures[3] as well as strategies based on microarray platforms, such as those developed by solution-based assays with nanoliter droplets in a microarray format.[4] Specific examples comprise aerosol deposition of reagents in nanoliter glycerol droplets,[5] nanoliter DMSO–water (9 : 1) droplets[6] and sub-nanoliter droplets assembled on PDMS microwell chips.[7]

However, these approaches suffer from complicated spotted droplet volume calibration procedures, require contact printing techniques and photolithographic masks, often employ solvents typically not compatible with enzymes (see below),[8] and show hurdles in performing multi-step reactions in a single experiment. In this scenario, we employed inkjet printing as one of the most promising methods for low-cost microarray fabrication since it does not require the use of masks, and given its ability to dispense 1–10 pL droplets with high throughput (10 spots s^{-1}) and positional accuracy by tuning fluid rheology and solid surface properties.[9] We proved the capability of such a technique to assay drug–target recognition in a simple microarray format. Droplets containing a model substrate (D-glucose)–inhibitor (D-glucal) couple were inkjet printed on a target enzymatic monolayer (glucose oxidase) linked to a functionalized silicon oxide solid surface and the competitive inhibition at the solid/liquid interface has been demonstrated.[10]

The described method, however, suffered from limitations due to the required covalent bond between the macromolecules and the solid support. This linkage is typically challenging for biomolecules since they might lose their function after covalent immobilization.[11] In order to address this problem, here we show a low-cost, ultra-small-volume, non-covalent array approach based on an inkjet printer for delivering multiple biomolecular systems in a multi-step/sequential picoliter droplets (water : glycerol = 7 : 3) assembly on solid surfaces. Biochemical reactions are conducted in such picoliter spots in a mid-throughput fashion, and the enzymatic inhibition is verified at the single spot level by luminometric detection. Liquid spots are stable during both the multilayer-assembling and the execution of the assay thanks to the high hygroscopicity of glycerol[12] which keeps a constant water content in the spots (Fig. S10–S11, ESI†). In particular, the deposited liquids contained all glycerol at 30% for optimizing drop rheological properties and resolving evaporation issues in droplets. Importantly, the detection sensitivity of such a Luminometric Sub-nanoliter Droplet-to-Droplet Array (LUMDA chip) may be increased by reducing the optical background through the employment of flat, antireflecting silicon oxide substrates (see Fig. S2, ESI†).

In this work, the reliability of the LUMDA chip is demonstrated with pharmacologically relevant systems such as CYP3A4, the most abundant liver-expressed membrane bound CYP450 enzyme and one of the most important enzymes responsible for the phase I drug metabolism.[13] Indeed, the lack

[a]*Scuola Superiore di Catania, Via Valdisavoia, 9 95123 Catania, Italy*
[b]*ST-Microelectronics, Stradale Primosole, 95123 Catania, Italy*
[c]*Dipartimento di Scienze Farmaceutiche e Biomediche, Università degli Studi di Salerno, Via Ponte don Melillo, 84084, Fisciano, Italy*
[d]*Dipartimento di Chimica ''S. Cannizzaro'', Università di Palermo, V.le delle Scienze, Parco d'Orleans II, 90128, Palermo, Italy.*
E-mail: bruno.pignataro@unipa.it

† Electronic supplementary information (ESI) available: Materials; methods; droplets microarray fabrication by inkjet printing; optimization of inkjetting process; effect of mechanical stresses upon CYP3A4 activity; multi-droplets microarray fabrication; optical calibration of the luminometric signal. See DOI: 10.1039/c2lc40948h

of adequate metabolic and pharmacokinetic parameters has been one of the main causes for the low number of new drugs approved by the US FDA in the past years. In this regard, early investigation of CYP450 mediated oxidative metabolism of a new chemical entity (NCE) represents the key for a successful drug discovery campaign. *In vitro* CYP450 assays represent a common approach for such investigations.[14] However, the majority of CYP450 inhibition studies are performed in multi-well plate formats with incubation volumes of 100–500 μL resulting in a high CYP450 consumption and high cost.

To this aim, we used the LUMDA chip for inhibition experiments on liposomes expressing CYP3A4 (see Fig. S1, ESI†). Firstly, we demonstrated the ability of the LUMDA chip to rank the IC_{50} profiling of two prototypical CYP3A4 inhibitors, namely ketoconazole and erythromycin.

Subsequently, the LUMDA chip has been employed to evaluate the CYP3A4 inhibitory potential of NCEs generated by combinatorial chemistry, showing similar chemical scaffolds and comparable physicochemical properties. In particular, we selected from a chemical library two compounds, namely TS51 and TS28 (Table S1, ESI† and Fig. 3), previously reported by one of us (S.C.) as inhibitors of two well-known CYP450 dependent enzymes, namely lanosterol 14 α-demethylase and aromatase.[15] Noteworthy, regardless of the presence of a common scaffold containing a central 1-amino-azole moiety and two identical aromatic portions, the LUMDA chip is able to distinguish their different pharmacological properties (see below). For comparison, the inhibitory effects of compounds were also investigated by conventional microwell plate formats coupled with fluorescence detection. The multilayer enzymatic droplets microarray was fabricated according to the scheme of Fig. 1a. Droplets containing different biochemicals were sequentially printed in the following order to form the spots (240 pL): (1) PBS buffer; (2) test inhibitor; (3) CYP3A4 liposomes plus enzymatic substrate (luciferin isopropyl-acetal – LIPA); (4) enzymatic regeneration system (glucose 6-phosphate dehydrogenase – G6PDH and glucose 6-phosphate – G6P). Then, we added to the array droplets containing luciferase + ATP for the optical quantification (Fig. 1b) to get a final 480 pL spot volume. Accordingly, luciferase catalyzes a bioluminescence reaction by D-luciferin leading to the production of photons increasing spot brightness (Scheme S1, ESI†). Arrays were fabricated in a 6 × 12 spot format with a spot-to-spot spacing of 500 μm (see also ESI†), thus leading to 72 spots usable for the assay including a reference spot per line (blanket spots) deriving from liposomes without CYP3A4. We also verified that final liquid spots were stable for more than 8 h without changing shape and volume (see Fig. S10, ESI†) allowing for dispensing the five array layers (Fig. S11, ESI,† 10–15 min), incubating (25 min) and saturating the kinetics processes (20–30 min). Thanks to the high-speed of the dispensing process (10 droplets s^{-1}) a high-throughput printing by thousands of multi-droplet spots in the same slide would be possible in 30–40 min and this could be improved by further automatization and the development of multi-nozzle cartridges.

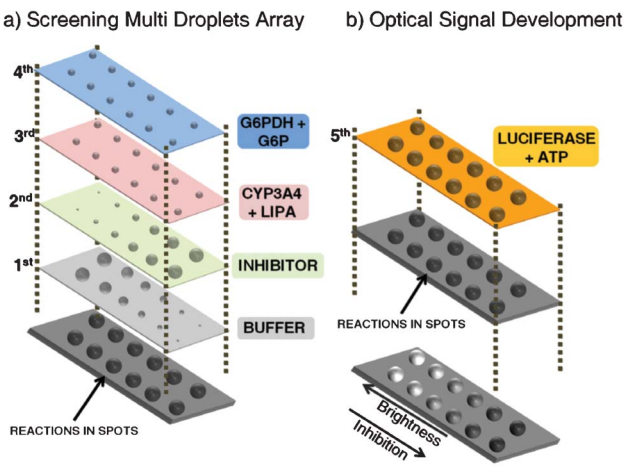

Fig. 1 Scheme of LUMDA-chip realization by piezoelectric dispensing of picoliter droplets on silicon dioxide solid supports: (a) layer-by-layer fabrication of the enzymatic array in presence of a concentration gradient of a test inhibitor molecule; (b) droplets of a mixture of luciferase and ATP are dispensed on the first microarray to get a final droplets array leading to an optical signal proportional to the enzymatic activity.

Accurate analysis of droplet dynamics was carried out by the stroboscopic imaging tool present in the Dimatix material inkjet printer (DMP-2800, Fujifilm) (see Fig. S4, ESI†). For all the experiments, a 11.52 μs pulse length waveform (Fig. S4a, ESI†) was used. Jetting voltage strongly affects droplet shape and droplet velocity. Interestingly, high jetting voltages (>24 V) were found to significantly affect CYP3A4 enzymatic activity (Fig. S6, ESI†), presumably due to the mechanical stresses at the nozzle exit together with droplet-to-droplet impact. In order to have enough droplet ballistic accuracy and avoid satellite droplets formation due to multiple breakups, ink jetting 10 pL droplets was performed at 18–20 V (5–6 m s^{-1}), whereas 1 pL droplets were dispensed at 9–10 V (9–10 m s^{-1}). Droplet-to-droplet addition was always executed under these optimized conditions (Fig. S5, ESI†). By these conditions it was possible to obtain droplets coalescence upon impact with a certain liquid mass movement under the impact site (*i.e.* condition of droplet spreading) but without the formation of liquid crowns.[16] Specifically, the spot area has been found to increase with the number of spot droplets, starting from about 3450 ± 400 μm^2 for the first layer to 6000 ± 620 μm^2 for the fourth layer. Note that after printing luciferase + ATP, the spot area increased up to 18 850 ± 770 μm^2 (*i.e.* 155 ± 31 μm spot diameter) such expansion due to the surfactant in the luciferase enzyme buffer used to slow down luminescence kinetics.

Likely, the spot roundness (ratio between the largest and the smallest circle containing the spot)[10] only slightly decreased starting from 0.951 ± 0.015 for the first layer, reaching 0.940 ± 0.029 for the fourth layer. Finally, luciferase + ATP layer printing led to 0.920 ± 0.020 which is still comparable to pin printing fabrication.[1] After the impact, complete merging of droplets occurs without any need of mixing steps, likely in less than one second.[17] Then, biomolecules diffuse across the entire spot with simultaneous occurrence of reactions. Molecular diffusion across the entire micrometer spot size would require some tens of seconds at the most.[18] This leads to a uniform spatial signal profile of the spots that we observe up to the saturation (20–30 min) in the pixel density map.

Since inkjet printing is a non-contact liquid dispensing method, droplet-to-droplet sequential addition in spots is easily controllable. Recently, pin printing methodologies have been

tentatively employed for droplet-to-droplet spots fabrication.[7] However such an approach is hampered by liquid upflowing from the spot to the pin with consequent contamination issues.

CYP450 enzymatic assays by luciferase bioluminescence[19] are conventionally performed by luminometer devices integrated in micro-well plate readers[20] with high enzyme consumption. Here, we implemented the luminance method in sub-nanoliter spots employing a digital camera calibrated to measure the absolute spot luminance by determining the relationship between luminance and the digital output level of the image (see Fig. S7–9, ESI†). Importantly, a thick (80 nm) silicon oxide layer has been employed for accurate spot luminance extraction, since native silicon oxide shows a higher optical background that compromises the readout of droplets of such a small size.

At first, we proved the suitability of the LUMDA chip for biochemical screening by arrays in which the CYP3A4 activity is measured as a function of concentration for a known inhibitor of this enzyme, namely ketoconazole.[21] After printing four different layers (buffer, inhibitor, CYP3A4 + LIPA, G6PDH + G6P) plus the luciferase + ATP layer, it was possible to fabricate spots with increasing ketoconazole concentration (0.042 μM, 0.42 μM, 0.25 μM, 0.36 μM, 0.75 μM) by adding at the spots an increasing number of droplets of drug solution as reported in Table S2, ESI.†

The optical integrated spot pixel density (I.D.; the product of area and mean gray value of the spot) significantly decreases with increasing ketoconazole concentration (Fig. 2a) following the inhibition of CYP3A4 mediated conversion of luciferin isopropyl-acetal to luciferin. In order to better observe the optical readout, the 3D output pixel intensity signal for each spot has been plotted inside a rectangle to extract the optical I.D. (Fig. 2b).

Student's *t*-test indicated no significant difference (95% confidence) among control spots containing all the employed systems without CYP3A4 (spot *g*) and spots showing the highest degree of CYP3A4 inhibition (spot *f*).

The good performance of the assay is proved by a measured quality *Z*-factor of 0.63 (a value higher than 0.5 indicates the suitability for high-throughput screening)[22] and an intra-array signal variability (I.D. coefficient of variation within one array) of about 4%. This last value is as good as that obtainable by fluorimetric detection methods on CYP3A4.[23] On the other hand, the inter-array signal variability (*i.e.* the coefficient of variation among different arrays) reaches 12%, such a value being ascribed to the different expression levels in recombinant enzyme liposome preparations.[19]

The CYP3A4 inhibition profiles obtained with the LUMDA chip for ketoconazole and erythromycin, another known inhibitor,[21] were compared. Fig. 3 shows the inhibition sigmoidal curves of ketoconazole (Fig. 3a) and erythromycin (Fig. 3b) showing R^2 respectively of 0.97645 and 0.93169. Moreover, the extracted IC_{50} from these experiments are 0.28 ± 0.02 μM for ketoconazole and 5.78 ± 0.42 μM for erythromycin. In agreement with conventional microwell assays, the LUMDA chip identifies ketoconazole as a stronger inhibitor of CYP3A4 than erythromycin.[24]

However, IC_{50} values from the LUMDA chip are significantly higher in comparison with the microwell assay, which furnished IC_{50} values of 0.061 μM and 4.8 μM for ketoconazole and erythromycin, respectively (Table S3, ESI†). This might be due to the reduction of enzymatic reaction rates in the viscous glycerol-rich medium which augments the contribution of molecular diffusion in the enzymatic kinetic control.[25] Noteworthy, while IC_{50} for ketoconazole is almost one order of magnitude higher than that obtained with microwell assays, inhibition by erythromycin occurs at much closer values. This might be due to the fact that conformational changes induced by ketoconazole binding to the secondary structure of CYP3A4 are larger than those induced by erythromycin.[21] Thus, due to the well-known glycerol ability to reduce protein flexibility,[26] in the case of ketoconazole higher ligand concentrations are required for the LUMDA chip with respect to conventional assays without glycerol. On the other hand, the addition of glycerol to the molecular ink allows decreasing drop surface tension as well

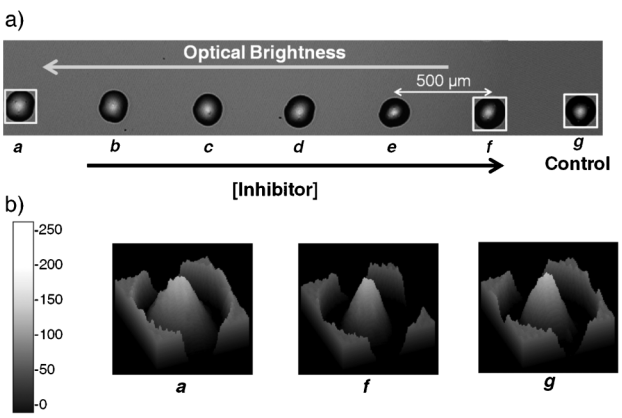

Fig. 2 (a) Optical image of a line of droplet-to-droplet spots. Whereas spot ***a*** does not contain inhibitor molecules, spots ***b*** to ***f*** contain increasing concentrations of ketoconazole. ***g*** is the control spot (*i.e.* liposomes which do not express CYP3A4). (b) 3D output pixel density of the spots.

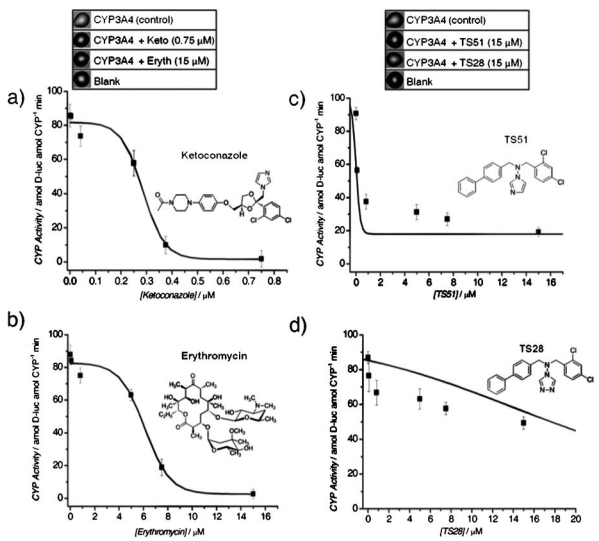

Fig. 3 Evaluation of compound activity on CYP3A4 by the LUMDA-chip platform. CYP3A4 inhibition by (a) ketoconazole, (b) erythromycin, (c) TS51, and (d) TS28 is reported. Each point is averaged by at least three different experiments. Enzymatic activity is expressed as attomoles of D-luciferin per attomoles of CYP3A4 per minute.

as increasing spot definition (see ESI†), and, importantly, drastically reduces the DMSO content (<0.06%). Indeed, DMSO is usually added (up to 5%) in conventional droplet microarrays[5,6] to alleviate evaporation issues and increase drug solubility. However the effects of solvents like DMSO on the protein activity make them incompatible with most enzymatic assays. In fact, owing to their lipophilic nature, organic solvents may alter the activities of the macromolecular targets directly by either modifying the native environment surrounding the proteins, by direct interaction with the macromolecular target or by protein denaturation, leading to misleading conclusions.[8] On the other hand, the polar solvent glycerol showed structural stabilizing properties and its effects on protein stresses by flux conditions may be neglected by optimizing the inkjet printing conditions (ESI† and ref. 9).

We then evaluated the ability of the LUMDA chip to discriminate between the CYP3A4 inhibitory activity of compounds TS51 and TS28 (Table S1, ESI†), previously reported as inhibitors of enzymes belonging to the CYP450 family.[15] Ketoconazole and erythromycin were used as inhibition positive controls. Despite the similar structures, these compounds show very different inhibition properties both in conventional and microarray assays. In particular, TS51 inhibits CYP3A4 with $IC_{50} = 1.15 \pm 0.03$ μM, whereas CYP3A4 activity results to be about 45 attomoles of D-luciferin per CYP3A4 per min at a TS28 concentration of 15 μM (about 44% less than the control, see Fig. 3d). Similarly, microwell plate assays show the same trend, thus corroborating the ability of LUMDA chips to discriminate between the activities of compounds with similar structures. In fact, while TS51 shows an IC_{50} of 0.097 μM, IC_{50} for TS28 is 6.730 μM. This is the first time that these inhibitors are tested with respect to CYP3A4 and the imidazole derivative (TS51) shows a drastically larger activity than the triazole one (TS28). Accordingly, a distinctive feature for inhibitor binding to CYP enzymes is the capability to interact as a sixth ligand with the iron atom of the heme group which is present in this enzyme family and the coordination can be performed by the lone pair carried on the sp^2 hybridized imidazole nitrogen in TS51 and with much less efficacy by other electron rich heterocycles such as triazole.[15]

In conclusion, we herein showed the establishment of a rapid multistep biological screening assay through non-immobilized molecules interacting in liquid sub-nanoliter droplets dispensed by piezoelectric inkjet printing and a luminometric detection method on substrates with optimized refractive index. As a perspective, the LUMDA chip can be applied to those systems for which covalent linking procedures to a surface decrease their activity. As a paradigmatic application, here we showed the use of the LUMDA chip to study the inhibition of the most important phase I metabolism enzymatic system, CYP3A4. We also validated the screening platform to determine the activity of structurally related compounds from a combinatorial library. As an alternative to luminometric detection, one can employ fluorescent detection to broaden the number of multiplexed biochemical assays to be performed on such a picoliter-spot scale. In the short term, this methodology will be an important prototype as a general approach since it can be extended to molecular and bio-molecular systems which show compatibility with moderate (20–30% v/v) concentrations of glycerol – realistically a large variety of biomolecular systems. This possibility makes the here shown methodology appealing not only for high-throughput screening of compound libraries, but also for other important fields such as single-cell assays, PCR, immunoassays, proteomics, catalysis and so on. Work to further integrate design software, printing hardware and control of chemical stimuli (pH, ionic strength, concentration gradients *etc.*) is currently underway in our laboratory.

Acknowledgements

We are grateful to Superlab (Consorzio Catania Ricerche) for his hospitality and to Giuseppe Francesco Indelli for the technical assistance in the development of the multi-layer inkjet printing dispensing. Domenico Timpano is acknowledged for his support in the set-up of the Luminometric assay detection. Italian MiUR programs (PRIN2008/20088L3BP3, FIRB-MERIT/RBNE08HWLZ010 and PONR&C2007-2013/PON02_00355_3416798) are acknowledged for funding.

References

1 G. Arrabito and B. Pignataro, *Anal. Chem.*, 2012, **84**, 5450.
2 P. J. Kitson, M. H. Rosnes, V. Sans, V. Dragone and L. Cronin, *Lab Chip*, 2012, **12**, 3267.
3 S. Fabiano and B. Pignataro, *Chem. Soc. Rev.*, 2012, **41**, 6859.
4 K. L. Aw, S. Q. Yao and M. Uttamchandani, *Methods Mol. Biol.*, 2010, **669**, 79.
5 D. N. Gosalia and S. L. Diamond, *Proc. Natl. Acad. Sci. U. S. A.*, 2003, **100**, 8721.
6 L. Mugherli, O. N. Burchack, L. A. Balakireva, A. Thomas, F. Chatelain and M. Y. Balakirev, *Angew. Chem.*, 2009, **121**, 7775, (*Angew. Chem., Int. Ed.*, 2009, **48**, 7639).
7 A. Binkert, P. Studer and J. Vörös, *Small*, 2009, **5**, 1070.
8 T. Arakawa, Y. Kita and S. N. Timasheff, *Biophys. Chem.*, 2007, **131**, 62.
9 G. Arrabito, C. Musumeci, V. Aiello, S. Libertino, G. Compagnini and B. Pignataro, *Langmuir*, 2009, **25**, 6312.
10 G. Arrabito and B. Pignataro, *Anal. Chem.*, 2010, **82**, 3104.
11 P. Jonkheijm, D. Weinrich, H. Schröder, C.M. Niemeyer and H. Waldmann, *Angew. Chem.*, 2008, **120**, 9762, (*Angew. Chem., Int. Ed.*, 2008, **47**, 9618).
12 R. A. Clark, P. B. Hietpas and A. G. Ewing, *Anal. Chem.*, 1997, **69**, 259.
13 K. S. Rabe, V.J. Gandubert, M. Spengler, M. Erkelenz and C. M. Niemeyer, *Anal. Bioanal. Chem.*, 2008, **392**, 1059.
14 R. Nicoli, R. Curcio, S. Rudaz and J.-L. Veuthey, *J. Med. Chem.*, 2009, **52**, 2192.
15 S. Castellano, G. Stefancich, R. Ragno, K. Schewe, M. Santoriello, A. Caroli, R. W. Hartmann and G. Sbardella, *Bioorg. Med. Chem.*, 2008, **16**, 8349.
16 A. L. Yarin, *Annu. Rev. Fluid Mech.*, 2006, **38**, 159.
17 A. M. Huebner, C. Abell, W. T. S. Huck, C. N. Baroud and F. Hollfelder, *Anal. Chem.*, 2010, **83**, 1462.
18 D. T. Chiu, R. M. Lorenz and G. D. M. Jeffires, *Anal. Chem.*, 2009, **81**, 5111.
19 J. J. Cali, A. Niles, M. P. Valley, M. A. O'Brien, T. L. Riss and J. Shultz, *Expert Opin. Drug Metab. Toxicol.*, 2008, **4**, 103.
20 U. Doshi and A. P. Li, *J. Biomol. Screening*, 2011, **16**, 903.
21 M. Ekroos and T. Sjögren, *Proc. Natl. Acad. Sci. U. S. A.*, 2006, **103**, 13682.
22 J. H. Zhang, T. D. Chung and K. R. Oldenburg, *J. Biomol. Screening*, 1999, **4**, 67.
23 S. M. Sukumaran, B. Potsais, M. Y. Lee, D. S. Clark and J. S. J. Dordick, *J. Biomol. Screening*, 2009, **14**, 668.
24 L. H. Cohen, M. J. Remley, D. Raunig and A. D. N. Vaz, *Drug Metab. Dispos.*, 2003, **31**, 1005.
25 B. B. Hasinoff and S. B. Chishti, *Biochemistry*, 1983, **22**, 58.
26 M. Gonnelli and G. B. Strambini, *Biophys. J.*, 1993, **65**, 131.

